molecular pharmaceutics

Article

pubs.acs.org/molecularpharmaceutics

Mathematical Modeling of PLGA Microparticles: From Polymer Degradation to Drug Release

Tommaso Casalini,*[,†] Filippo Rossi,[†] Stefano Lazzari,[‡] Giuseppe Perale,[§,∥] and Maurizio Masi[†]

[†]Dipartimento di Chimica, Materiali ed Ingegneria Chimica "Giulio Natta", Politecnico di Milano, via Mancinelli 7, 20131 Milano, Italy

[‡]Institute for Chemical and Bioengineering, Department of Chemistry and Applied Biosciences, ETH Zurich, Vladimir-Prelog-Weg 1, 8093 Zurich, Switzerland

[§]Department of Innovative Technologies, University for Applied Science and Art of Southern Switzerland, via Cantonale 2c, CH-6928 Manno, Switzerland

[∥]Swiss Institute for Regenerative Medicine, via ai Söi, CH-6807 Taverne, Switzerland

Supporting Information

ABSTRACT: The present work is focused on the development and the validation of a mechanistic model describing the degradation of drug-loaded polylactic-*co*-glycolic acid microparticles and the drug release process from such devices. Microparticles' degradation is described through mass conservation equations; the application of population balances allows a detailed description of the hydrolysis kinetics, which also takes into account the autocatalytic behavior that characterizes bulk eroding polymers. Drug release considers both drug dissolution and the diffusion of dissolved active principle through the polymeric matrix. The diffusion of oligomers, water, and drug is assumed to follow Fickian behavior; the use of effective diffusion coefficients takes into account the diffusivity increase due to polymer hydrolysis. The model leads to a system of partial differential equations, solved by means of the method of lines. The model predictions satisfactorily match with different sets of literature data, indicating that the model presented here, despite its simplicity, is able to describe the key phenomena governing the device behavior.

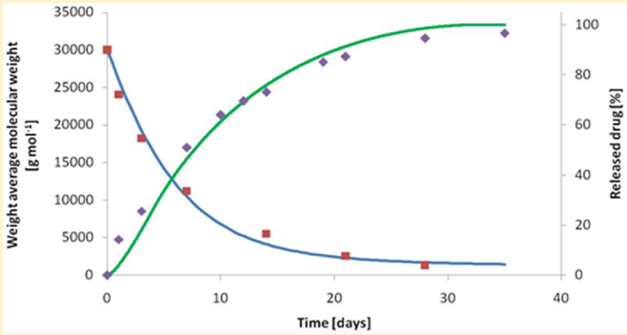

KEYWORDS: *mathematical modeling, drug release, microparticles, biopolymers, polyesters*

INTRODUCTION

In the drug delivery field, aliphatic polyesters are common materials for bioresorbable devices, such as microparticles, which are the object of study in the present article. Polymers like polylactic acid (PLA), polyglycolic acid (PGA), poly-ε-caprolactone (PCL), and their copolymers, such as poly lactic-*co*-glycolic acid (PLGA), are commonly employed in a wide range of medical devices thanks to their interesting properties.[1−3]

Starting from the 1970s, when the first bioresorbable suture threads were developed,[3] aliphatic polyesters are now widely studied as devices for the controlled release of drugs, growth factors, and proteins.[1,4−9]

Such materials naturally degrade in *in vivo* environments because of the hydrolysis mechanism, thus avoiding surgical operations for device removal and improving patients' recovery. As device degradation proceeds, the loaded active principle can diffuse through the matrix, reaching the target tissue or the systemic circulation.

Generally speaking, device behavior in terms of both degradation and release characteristic times is the result of the synergic effect of several phenomena.[10−12] Polymer degradation involves several mechanisms. Polymer hydrophilicity/hydrophobicity and crystallinity determine the water uptake and thus hydrolysis dynamics; indeed, hydrophilic and amorphous materials can retain a greater amount of water and thus are subjected to a faster degradation. Water uptake is also influenced by molecular weight; the initial amount of adsorbed water decreases as the molecular weight of undegraded device increases.

As mentioned, polymer degradation occurs due to the hydrolysis mechanism: water penetrates into the matrix and breaks ester bonds, which constitute the polymer backbone. The resulting oligomers can diffuse in and out of the matrix and act as a catalyst for the hydrolysis reaction because of their carboxyl groups, as degradation is enhanced in acid environments.[10,13] Moreover, loaded active ingredients can interfere with hydrolysis, speeding or slowing the process depending on the

Received: January 24, 2014
Revised: June 12, 2014
Accepted: September 17, 2014
Published: September 17, 2014

ACS Publications © 2014 American Chemical Society

specific interactions with the reaction.[10,14,15] The dynamics of both water diffusion and hydrolysis regulate the degradation mechanism. On one hand, if the characteristic time of water penetration into the matrix is lower than the depolymerization one, then homogeneous or bulk degradation takes place since the entire matrix is subjected to hydrolysis reaction. In contrast, if ester bonds are hydrolyzed faster than water diffusion, heterogeneous or surface degradation occurs; only the surface is subjected to degradation, while the bulk remains intact. Currently, it is widely accepted that the degradation mechanism also depends on device geometry. Von Burkersroda[16] introduced a critical thickness to decide upon the degradation mechanism: when the device characteristic length is above the critical thickness, surface erosion occurs, whereas bulk erosion takes place otherwise. Notably, bulk-eroding materials may transition from homogeneous degradation to heterogeneous degradation when the autocatalytic effects are significant at the center of the material due to extended diffusion length.[17]

Drug release depends on drug dissolution (since only solubilized drugs diffuse) and diffusion through the matrix. The dissolution dynamics is primarily influenced by the solubilization limit (which decreases as drug hydrophobicity increases) and crystallite dimensions, which determines the specific surface available at the water/drug interface. In more complex situations, drug solubility can be also affected by the presence of different crystalline and hydrate forms and recrystallization phenomena.[12] If the active ingredient is loaded into a bioresorbable matrix, the release rate is also influenced by device degradation. As hydrolysis proceeds, new and wider diffusion paths are created since polymer chains become smaller and more distant from each other; the overall result is thus a dynamic increase of drug diffusivity in the matrix.

The good overview of the most relevant involved phenomena and their synergic effect in the overall device behavior resulted in a sparkling research activity in the mathematical modeling field, as recently reviewed by several authors,[18−21] aimed at providing a reliable quantitative description of polymer degradation and drug release.

Literature offers many examples of mathematical models, based on deterministic[22−26] or stochastic[27−29] approaches, with a lumped[22−24,26] or detailed[25,30−36] description of hydrolysis kinetics. Device degradation can be coupled with drug release; drug diffusion is usually assumed to follow Fickian behavior.[37,38] In order to describe the interplay of device hydrolysis and diffusivity, diffusion coefficients can be related to monomer concentration,[27] molecular weight,[33,34,39] or porosity.[23,26,28]

In this framework, we developed a mathematical model focusing our attention on polymeric microparticles. Among the existing devices, PLGA-based microparticles gained a relevant role because they combine a variety of interesting features, such as a good biocompatibility and biodegradability, a tunable release rate,[5,40] the encapsulation of hydrophobic drugs, which otherwise would possess a poor oral bioavailability,[41] and an easy administration through injection or oral ingestion.[5]

Degradation phenomena are described through mass conservation equations, by means of population balances, which allow a detailed treatment of chain hydrolysis. The autocatalytic effect is explicitly taken into account, assuming a degradation rate proportional to the concentration of acidic moieties. Mass balances also take into account diffusion phenomena (assumed as Fickian) since the resulting oligomers can diffuse through the matrix and their local concentration determines the hydrolysis enhancement due to autocatalytic effects.

Drug release is described taking into account both the solubilization dynamics of drug crystallites and the diffusion of the dissolved active principle through the matrix. The diffusion coefficients of the involved species (oligomers, water, and drug) are expressed as a function of the average molecular weight, thus reproducing the diffusion enhancement along the degradation reaction.

One of the most interesting peculiarities of the model derives from the coupling of device degradation and drug release since these phenomena are connected to each other.[42] As mentioned, polymer hydrolysis creates new and wider diffusive paths, which implies a dynamic enhancing of drug diffusivity within the matrix. In literature, drug diffusion is usually described through the analytical or numerical solution of Fick's second law, fitting an apparent diffusion coefficient, which implicitly contains the effect of both device degradation and drug dissolution.[18] The here proposed model aims at overcoming such limits, offering a more complete and detailed view of the involved phenomena and their mutual interactions. This approach has been validated with independent sets of experimental data taken from the literature, involving microparticles' degradation[43−45] and release of paclitaxel,[43] lidocaine,[44] and ibuprofen.[45]

■ MODEL DEVELOPMENT

All simulations are referred to a surrounding environment constituted by a phosphate buffer saline solution (pH 7.4) with a temperature of 37 °C. The polymeric microparticles are modeled as a sphere of constant volume with radial variations in concentrations, being subjected to bulk degradation since their diameter is below the theoretical critical threshold above which surface degradation becomes dominant (7.4 cm for aliphatic polyesters). Moreover, experimentally, aliphatic polyesters of all sizes are known to undergo bulk degradation in physiological relevant conditions.[16]

The model only considers a radial coordinate, as the particles are assumed to be perfect spheres. The microspheres diameter distribution is not taken into account; calculations are carried out assuming that all particles have the same size, whose value is equal to their mean diameter.[32]

Polymer degradation, due to acid-catalyzed hydrolysis mechanism, is described according to the following kinetic scheme:[46]

$$P_{n+m} + W + H^+ \Rightarrow P_n + P_m + H^+ \tag{1}$$

The influence of the loaded active ingredient on polymer degradation is not treated explicitly in the model, but its effect, if present, is implicitly contained in the hydrolysis kinetic constant. The PLGA copolymer is described as a homopolymer, with a pseudomonomeric unit whose molecular weight is a composition-weighted average between lactide and glycolide units.

Water molecules penetrate inside the matrix and break long polymeric chains into small oligomers, which can diffuse through and out of the matrix. The aforementioned kinetic scheme is described in detail by means of mass conservation equations, by coupling population balances[47] with a reaction−diffusion approach. In particular, only the diffusion of oligomers with a chain length up to 9 units is taken into account, as suggested by Batycky et al.[32] In order to reproduce the autocatalytic effect, which characterizes bulk eroding biopolymers, the degradation rate is proportional to the overall carboxyl moieties concen-

tration (and thus to the polymer concentration). The water diffusion inside the matrix also causes the solubilization of the loaded active ingredient, whose dynamics depends on drug loading and its solubilization limit. If the drug concentration is higher than the solubilization limit, dissolution dynamics must be taken into account, while this phenomenon can be reasonably considered instantaneous (and thus neglected) if the drug amount is well below solubilization limit.[33,34]

Polymer Degradation. According to kinetic eq 1, a water molecule breaks one long chain in two smaller fragments; among the degradation products, only water and oligomers up to nonamers diffuse inside the matrix, whereas longer chains are assumed to be nondiffusing. These assumptions allow writing mass conservation equations for the monomer (eq 2.a), the diffusing oligomers (with a chain length comprised between 2 and 9, eq 2.b), polymer chains (with a number of monomeric units equal or higher than 10, eq 2.c) and water (eq 2.d), respectively:

$$\frac{\partial C_M}{\partial t} = \frac{1}{r^2}\frac{\partial}{\partial r}\left(D_M r^2 \frac{\partial C_M}{\partial r}\right) + 2k_d C_w \sum_{j=2}^{\infty} C_j \sum_{j=1}^{\infty} C_j \tag{2.a}$$

$$\frac{\partial C_n}{\partial t} = \frac{1}{r^2}\frac{\partial}{\partial r}\left(D_n r^2 \frac{\partial C_n}{\partial r}\right) + 2k_d C_w \sum_{j=n+1}^{\infty} C_j \sum_{j=1}^{\infty} C_j - (n-1)k_d C_w C_n \sum_{j=1}^{\infty} C_j \quad 2 \le n \le 9 \tag{2.b}$$

$$\frac{\partial C_n}{\partial t} = 2k_d C_w \sum_{j=n+1}^{\infty} C_j \sum_{j=1}^{\infty} C_j - (n-1)k_d C_w C_n \sum_{j=1}^{\infty} C_j \quad n > 9 \tag{2.c}$$

$$\frac{\partial C_w}{\partial t} = \frac{1}{r^2}\frac{\partial}{\partial r}\left(D_w r^2 \frac{\partial C_w}{\partial r}\right) - k_d C_w \sum_{j=2}^{\infty} (j-1) C_j \sum_{j=1}^{\infty} C_j \tag{2.d}$$

where C_M, C_n, and C_w are the molar concentrations of monomer, polymer chains of length n, and water, respectively; D_M, D_n, and D_w are diffusion coefficients for monomer, diffusing oligomers, and water, respectively; r is the microparticle radius, and k_d is the degradation kinetic constant. The model assumes that diffusion follows Fickian behavior; diffusion coefficients are included into the derivative operator since they depend on molecular weight, which varies along the radius as hydrolysis takes place.

Since the degrading polymer chains may consist of up to 10^4–10^5 units, it would be necessary to solve a quite large number of differential equations (eq 2.c). Therefore, the method of moments is applied for $n > 9$, reducing the population balance (eq 2.c) to three equations: the statistical moments of order zero, one, and two. The generic kth order statistical moment is defined as follows:[47]

$$\mu_k = \sum_{n=1}^{\infty} n^k C_n \tag{3}$$

Monomer, oligomers and water mass balances can be reformulated in terms of statistical moments:

$$\frac{\partial C_M}{\partial t} = \frac{1}{r^2}\frac{\partial}{\partial r}\left(D_M r^2 \frac{\partial C_M}{\partial r}\right) + 2k_d C_w(\mu_0 - C_M)\mu_0 \tag{4.a}$$

$$\frac{\partial C_n}{\partial t} = \frac{1}{r^2}\frac{\partial}{\partial r}\left(D_n r^2 \frac{\partial C_n}{\partial r}\right) + 2k_d C_w\left(\mu_0 - \sum_{j=1}^{n} C_j\right)\mu_0 - (n-1)k_d C_w C_n \mu_0 \quad 2 \le n \le 9 \tag{4.b}$$

$$\frac{\partial C_w}{\partial t} = \frac{1}{r^2}\frac{\partial}{\partial r}\left(D_w r^2 \frac{\partial C_w}{\partial r}\right) - k_d C_w(\mu_1 - \mu_0)\mu_0 \tag{4.c}$$

By applying the definition of kth order moment, three partial differential equations describing the time evolution of statistical moments can be obtained:

$$\frac{\partial \mu_0}{\partial t} = \sum_{j=1}^{9} \frac{1}{r^2}\frac{\partial}{\partial r}\left(D_j r^2 \frac{\partial C_j}{\partial r}\right) + k_d C_w(\mu_1 - \mu_0)\mu_0 \tag{5.a}$$

$$\frac{\partial \mu_1}{\partial t} = \sum_{j=1}^{9} \frac{j}{r^2}\frac{\partial}{\partial r}\left(D_j r^2 \frac{\partial C_j}{\partial r}\right) \tag{5.b}$$

$$\frac{\partial \mu_2}{\partial t} = \sum_{j=1}^{9} \frac{j^2}{r^2}\frac{\partial}{\partial r}\left(D_j r^2 \frac{\partial C_j}{\partial r}\right) + \frac{k_d C_w \mu_0}{3}\left(\mu_1 - 2\frac{\mu_2^2}{\mu_1} + \frac{\mu_2 \mu_1}{\mu_0}\right) \tag{5.c}$$

Statistical moment-based approaches proved to give a satisfactory description of degradation phenomena, as already presented in our previous works.[30,31,33,34,48]

These three partial differential equations substitute for the large number of differential eqs (10^4–10^5) needed to describe the concentration time evolution of polymer chains with a chain length equal to or higher than 10. Statistical moments allow computing average properties of interest such as polydispersity and molecular weight, whose spatial and temporal evolution influence the effective diffusion coefficient. Moreover, the moments of the first three orders have a physical meaning: the zeroth order moment is equal to the overall polymer concentration per unit volume, the first order moment represents the overall concentration of monomeric units per unit volume, and the second order moment is related to polymer polydispersity. Concerning boundary conditions, the symmetry of water, monomer, and oligomer concentration profiles is imposed at the microparticle center, while at the microparticle/environment interface the mass transfer resistance at the particle surface is taken into account:

$$-D_i(r = R)\left.\frac{\partial C_i}{\partial r}\right|_{r=R} = k_{C,i}^{ext}(C_{b,i} - C_i(r = R)) \quad i = \text{water, monomer, oligomers} \tag{6}$$

where $C_{b,i}$ is the ith species concentration in the bulk phase of surrounding environment and $k_{C,i}^{ext}$ is the ith species mass transfer coefficient. Such value is equal to 0 for monomer and oligomers and to 0.055 mol cm^{-3} for water. This is consistent with the periodic removal of the surrounding constituted by water.

Initial conditions for water, monomer, and oligomers consider a null concentration since microparticles are supposed to be anhydrous and without residual short chains. Initial conditions for statistical moments are referred to nondegraded polymer. Details about the employed equations and their derivation are given in the Supporting Information.

Table 1. Simulation Input Data for Drug-Free and Lidocaine-Loaded Microparticles; Experimental Data Taken from Siepmann et al.[44]

	drug-free particles		lidocaine-loaded particles	
radius (μm)	7.9	55	7.2	53
MW_{mon} (g mol^{-1})	83	83	83	83
ρ_{pol} (g cm^{-3})	1.2	1.2	1.2	1.2
MW_w (g mol^{-1})	29310	29050	31830	32440
PD	1.6	1.6	1.6	1.6
D_{olig}^0 (cm^2 s^{-1})	1×10^{-10}	1×10^{-10}	1×10^{-10}	1×10^{-10}
D_W^0 (cm^2 s^{-1})	1×10^{-8}	1×10^{-8}	1×10^{-8}	1×10^{-8}
D_D^0 (cm^2 s^{-1})[a]			3.972×10^{-14}	1.324×10^{-12}
$D_{D,eff}^0$ (cm^2 s^{-1})[a]			9.146×10^{-15}	3.107×10^{-13}
$k_{C,D}^{int}$ (s^{-1})[a]			5.635×10^{-5}	4.682×10^{-5}
$C_{D,lim}$ (mol cm^{-3})[b]			2.791×10^{-5}	2.791×10^{-5}
drug load (% w/w)			4	4
k_d (mol^{-2} cm^6 s^{-1})[a]	1.386×10^{-3}	1.673×10^{-3}	2.125×10^{-3}	3.287×10^{-3}

[a]Fitted from experimental data. [b]Taken from ref 51.

Table 2. Simulation Input Data for Ibuprofen-Loaded and Paclitaxel-Loaded Microparticles; Experimental Data Taken from Klose et al.[45] and Elkharratz et al.[43]

	Klose et al.[45] ibuprofen-loaded particles		Elkharratz et al.[43] paclitaxel-loaded particles	
radius (μm)	13	57.5	9.4 (with DENA)	9.4 (without DENA)
MW_{mon} (g mol^{-1})	83	83	83	83
ρ_{pol} (g cm^{-3})	1.2	1.2	1.2	1.2
MW_w (g mol^{-1})	35170	34050	40000	40000
PD	1.6	1.6	1.6	1.6
D_{olig}^0 (cm^2 s^{-1})	1×10^{-10}	1×10^{-10}	1×10^{-10}	1×10^{-10}
D_W^0 (cm^2 s^{-1})	1×10^{-8}	1×10^{-8}	1×10^{-8}	1×10^{-8}
D_D^0 (cm^2 s^{-1})[a]	3.424×10^{-10}	3.926×10^{-9}		2.378×10^{-12}
$D_{D,eff}^0$ (cm^2 s^{-1})[a]	3.043×10^{-13}	2.185×10^{-12}		7.04×10^{-15}[c]
$k_{C,D}^{int}$ [s^{-1}][a]	4.635×10^{-2}	2.896×10^{-2}		8.463×10^{-5}
$C_{D,lim}$ (mol cm^{-3})[b]	1.170×10^{-7}	1.170×10^{-7}		0.6×10^{-6}
drug load (% w/w)	4	4		18
k_d (mol^{-2} cm^6 s^{-1})[a]	2.016×10^{-3}	3.197×10^{-3}	5.571×10^{-3}	4.062×10^{-4}

[a]Fitted from experimental data. [b]Taken from refs 52 (ibuprofen) and 53 (paclitaxel). [c]Fitted assuming a nonuniform initial drug distribution.

Drug Release. Concerning drug release, the model assumes that the drug is uniformly distributed inside the matrix and diffuses according to Fick's law. It is also assumed that drug molecules are not affected by the pH value inside the matrix, i.e., the local acidic environment has no influence on the active ingredient stability, but only on its protonation state. The release mechanism dynamics is described as follows: water penetrates inside the polymeric matrix and wets drug crystals, allowing the dissolution of the active ingredient, which diffuses through the microparticle. Thus, two mass balances are required, for the loaded and the dissolved drug, respectively:

$$\frac{\partial C_{D,load}}{\partial t} = -k_{C,D}^{int}(C_{D,lim} - C_{D,sol}) \tag{7.a}$$

$$\frac{\partial C_{D,sol}}{\partial t} = k_{C,D}^{int}(C_{D,lim} - C_{D,sol}) + \frac{1}{r^2}\frac{\partial}{\partial r}\left(D_D r^2 \frac{\partial C_{D,sol}}{\partial r}\right) \tag{7.b}$$

where $C_{D,load}$ and $C_{D,sol}$ are the molar concentration of the loaded and the solubilized drug, respectively, $C_{D,lim}$ is the drug solubilization limit, $k_{C,D}^{int}$ is the mass transfer coefficient related to drug crystallites inside the polymeric matrix, and D_D is the diffusion coefficient of the active ingredient in the device. In particular, eq 7.a represents the dissolution rate of drug crystals, described through the Noyes–Whitney equation.[49] It is assumed that only one drug solid phase exists and that no significant recrystallization occurs during drug release. It must be pointed out that $k_{C,D}^{int}$ is a lumped parameter since it contains the influence of drug crystallites dispersion (that is, the number of drug particles per unit volume) and characteristic dimension, which determines the specific surface available for dissolution.

For the dissolved drug, one boundary condition imposes a concentration profile symmetry at the microparticle center, while at the microparticle/environment interface the mass transfer resistance at particle surface is taken into account (eq 6); drug bulk concentration is equal to 0, in order to reproduce the periodic removal of surrounding water. The initial value of solubilized drug is equal to zero, while the initial value of loaded drug is determined by the effective drug loading, considering, as said, a uniform active ingredient dispersion through the matrix.

Model Parameter Estimation. The involved parameters are essentially related to polymer degradation phenomena and transport phenomena inside the polymeric matrix. Because the model is based on first-principles, such quantities have a specific physical meaning (kinetic constants, diffusion coefficients, and so on) and thus can be independently and robustly estimated from experimental data.

The hydrolysis kinetic constant k_d is fitted from experimental data, from time evolution of weight-average molecular weight. As for diffusion coefficients, the model assumes an expression that

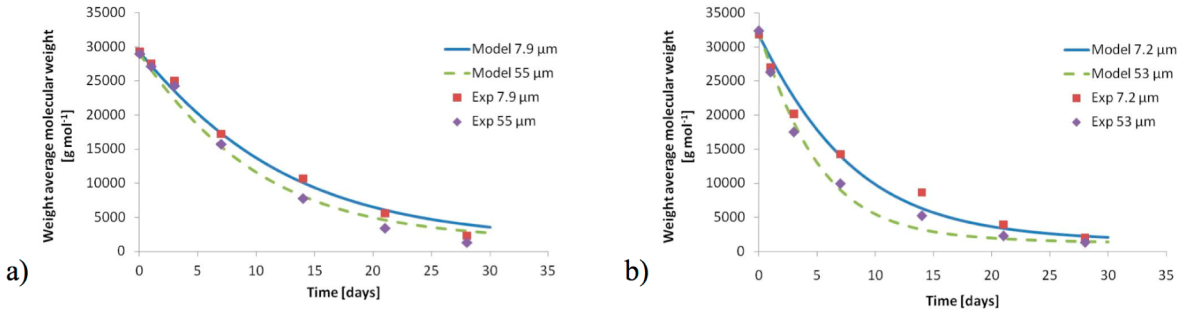

Figure 1. Experimental (squares and diamonds) and predicted (continuous and dashed lines) molecular weight loss for drug-free (a) and drug-loaded (b) microparticles. Size values refer to microsphere radii. Experimental data taken from Siepmann et al.[44]

takes into account the diffusivity increase as hydrolysis occurs through time and spatial evolution of number-average molecular weight MW_n, as presented in our previous works:[33,34]

$$D_i = D_i^0 \exp\left[2.5\left(1 - \frac{MW_n(t, r)}{MW_n(t = 0)}\right)^{0.5}\right] \quad i \leq 9 \tag{8}$$

where D_i^0 is the diffusion coefficient of the ith oligomer (including monomeric units) before the degradation onset.

Note that eq 8 is also employed to describe the diffusivity of both water and drug. This functional form was used for all simulation performed.

Number-average molecular weight can be computed from statistical moments:

$$MW_n = \frac{\mu_1}{\mu_0} MW_{mon} \tag{9}$$

where MW_{mon} is the monomer molecular weight.

Both D_{drug}^0 and $k_{C,D}^{int}$ are estimated from *in vitro* release data. Since the number-average molecular weight depends on both time and space, D_i must be included into the spatial derivative operator that appears in the mass balances. The mass transfer coefficient for the ith species $k_{C,i}^{ext}$, related to the microparticle surface and the external surrounding environment, is evaluated from the Sherwood number, which is equal to 2 for spherical systems in stagnant conditions:[50]

$$Sh = 2 = \frac{2k_{C,i}^{ext}R}{D_i} \tag{10}$$

All input parameters used in the simulations are reported in Tables 1 and 2.

NUMERICAL SOLUTION

The proposed equations constitute a single system that describes the synergic effects of all involved phenomena. In an *in vitro* environment, diffusion phenomena (and thus drug release) are influenced by polymer degradation, which depends on the local concentration of both water and diffusing oligomer chains.

The obtained system of partial differential equations has been solved applying the method of lines:[54] spatial derivatives are approximated through finite differences by means of a centered formulation. The resulting system of ordinary differential equations (ODE) (where time is now the only independent variable) is then numerically integrated with the *ode15s* algorithm as implemented in MATLAB. The fitting procedure has been performed through the Levenberg−Marquardt algorithm as implemented in MATLAB. The overall ODE number is equal to 15np, where np is the number of discretization points of the spatial coordinate; np values range from 200 to 400 and have been chosen so that the error related to drug release is kept below 0.5% during integration. Error estimation, concerning both polymer degradation and drug release, has been carried out by means of mass balances; details are reported in the Supporting Information. The required CPU time ranges from 1 to 5 min on a common laptop, according to the chosen np value and the simulated time span; computational efficiency has been greatly improved through *JPattern* command implemented in MATLAB, which takes advantage of the sparsity of Jacobian matrix.

RESULTS AND DISCUSSION

Lidocaine-Loaded Microparticles. Siepmann et al.[44] characterized the degradation of both drug-free and lidocaine-loaded microparticles having different particle radii, between 7.2 and 55 μm. The authors described hydrolysis kinetics with a simple pseudo-first order model:

$$MW_w(t) = MW_0 \exp(-k_{deg}t) \tag{11}$$

where MW_w is weight-average molecular weight, MW_0 is the initial molecular weight of undegraded device, t is time, and k_{deg} is degradation rate constant.

In particular, the degradation rate constants increase as the size of the microspheres increases, suggesting an autocatalytic effect. As shown in Figure 1, the model presented here is able to quantitatively predict the molecular weight decrease for both drug-free and drug-loaded devices; for the sake of clarity, only results involving the smallest and the largest microspheres are here presented. The initial weight-average molecular weight MW_w of each particle is listed in Table 1. All other plots show a good agreement with experimental data, and fitted constants are consistent among each other. For the sake of completeness, omitted data are reported in the Supporting Information.

As microsphere size increases, degradation kinetic constants increase as well, from 1.386×10^{-3} to 1.673×10^{-3} cm^6 mol^{-2} s^{-1} for drug-free particles and from 2.125×10^{-3} to 3.287×10^{-3} cm^6 mol^{-2} s^{-1} for drug-loaded particles. Generally speaking, hydrolysis constants for drug-loaded microparticles can be seen as "lumped" parameters since they implicitly account for the drug effect on the degradation kinetic mechanism. In this case, hydrolysis constants are slightly higher for lidocaine-loaded microspheres than for drug-free ones, suggesting a present but limited influence of the active ingredient on device degradation behavior.[10,14] Moreover, for both drug-free and drug-loaded particles, the kinetic constant increases as the microsphere radius increases, underlining the connection between device size and autocatalytic effect.

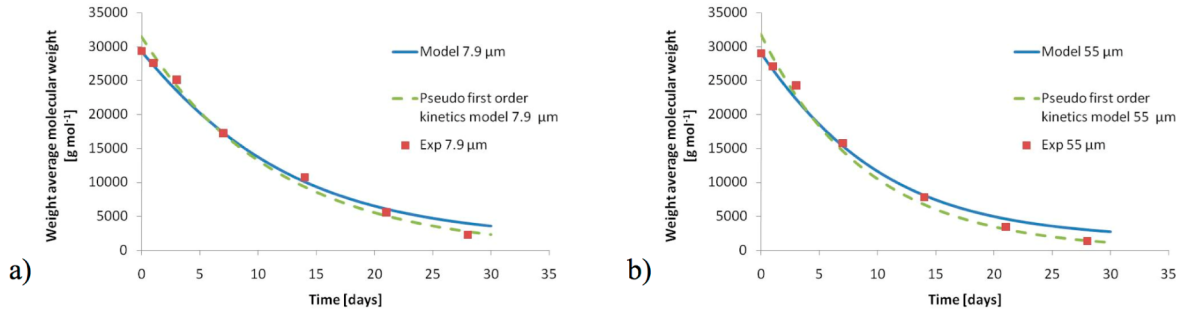

Figure 2. Comparison between detailed model (continuous line) and the pseudo first order kinetics model (dashed line) prediction of molecular weight loss for 7.9 μm (a) and 55 μm (b) microparticles. Experimental data (squares) taken from Siepmann et al.[44]

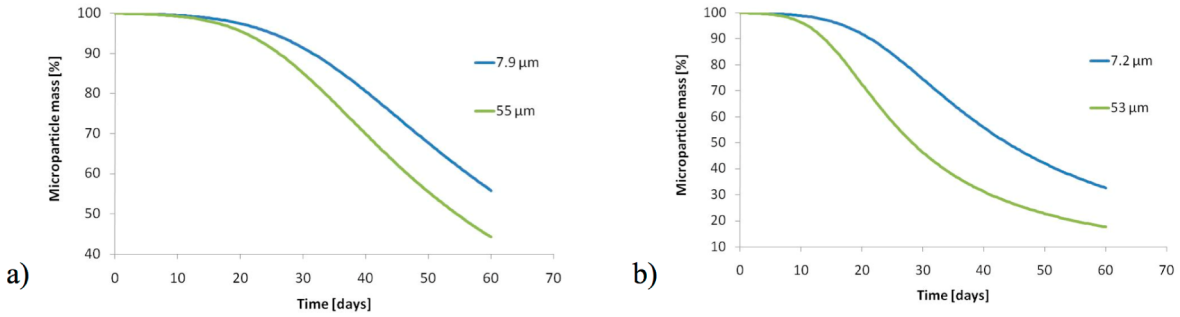

Figure 3. Predicted mass loss for drug-free (a) and lidocaine-loaded (b) microparticles.

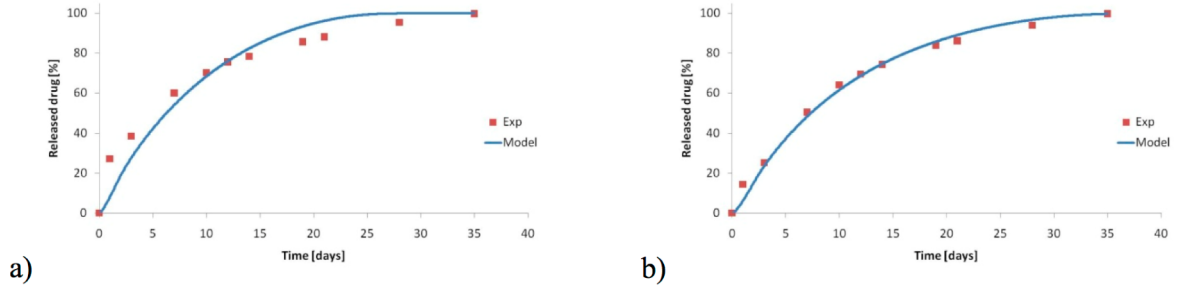

Figure 4. Experimental (squares) and predicted (continuous lines) release profiles for 7.2 μm microparticles (a) and 53 μm microparticles (b). Experimental data taken from Siepmann et al.[44]

A comparison between the time evolution of weight-average molecular weight obtained through the here proposed model and a pseudo first order kinetics model is shown in Figure 2. It can be seen that these two models lead to comparable results; the main difference lies in the modeling approach. A pseudo first order kinetics model is useful for a preliminary quantitative evaluation of device degradation, but it lacks a high enough level of detail to offer insights about mass loss or concentration profiles of the hydrolysis products. In contrast, the here proposed model allows a detailed characterization of microparticle behavior, and being based on first-principles, it can be used to obtain quantitative predictions.

The predicted mass loss rate (Figure 3) increases as size increases. Although oligomers experience longer diffusive paths, autocatalysis accelerates the degradation kinetics and therefore particles' porosity, thus enhancing the mass loss rate. This explanation is consistent with the data presented by Siepmann et al. regarding lidocaine release from such devices: experimental release rate has not a strong dependence on microsphere size, suggesting that the effect due to longer diffusive paths is balanced by a more pronounced porosity and thus diffusivity increases. This is not intuitive since diffusive paths increase as particle radius increases and slower rates for big devices would be expected.

The time evolution of mass loss can be divided in two different phases. In the first one, a relevant molecular weight decrease (Figure 2) is coupled with a negligible or null mass loss (Figure 3); even though degradation takes place and polymer chains are hydrolyzed in smaller fragments, there is only a negligible fraction of water-soluble oligomers that diffuses and leaves the matrix. During the second phase, there is an increased production of small oligomers due to the degradation of small fragments, which causes the attainment of the mass loss.

For the description of lidocaine release, a comparison between experimental data and the calculated release profile is represented in Figure 4; again, for the sake of clarity, only results involving the smallest radius (7.2 μm, Figure 4a) and the largest radius (53 μm, Figure 4b) are here presented, while all plots are available in the Supporting Information. The model adequately reproduces the experimental trend and thus provides a good description of the synergic effects of solubilization dynamics, drug diffusion, and porosity increase due to degradation.

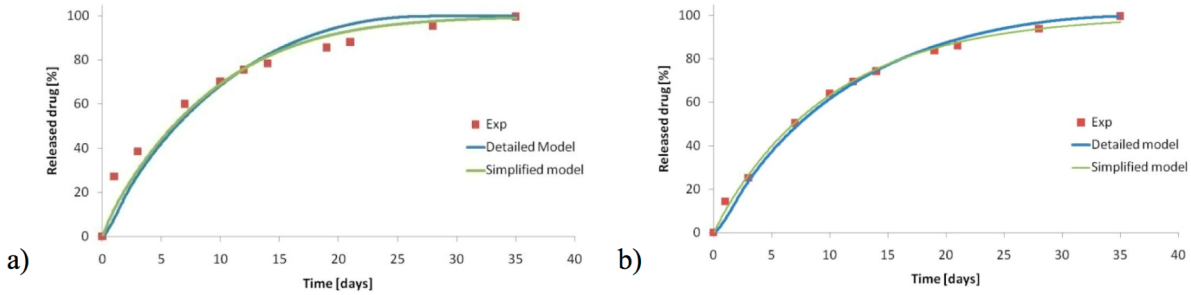

Figure 5. Comparison between detailed and simplified drug release description for 7.2 μm microparticles (a) and 53 μm microparticles (b). Experimental data (squares) taken from Siepmann et al.[44]

Experimental data fitting provided solubilization constant k_C^{int} values equal to 5.635×10^{-5} and 4.682×10^{-5} s^{-1} and diffusion coefficient D_{drug}^0 values equal to 3.972×10^{-14} and 1.324×10^{-12} cm^2 s^{-1} for 7.2 and 53 μm devices, respectively. For the solubilization constants, it can be seen that the values are quite similar; this indicates that the distribution and the dimension of drug crystallites in the matrix are not affected by the microparticle size. In contrast, the diffusion coefficient increases as microsphere radius increases. This trend reflects once more how in larger particles the longer diffusive paths are balanced by an enhanced porosity increase (due to a more pronounced autocatalytic effect). In other words, diffusion cannot be decoupled from reaction: a reasonable expression to account for this interdependency is given by eq 9, although the fitting results suggest that this is not yet the "universal" relationship, as otherwise the diffusion coefficient should have been size-independent.

Notably, a further increase of the solubilization constant has no influence on the release behavior. Such evidence can be explained by defining the solubilization (τ_{sol}) and diffusion (τ_{diff}) characteristic times, as follows:

$$\tau_{sol} = \frac{1}{k_{C,D}^{int}} \tag{12}$$

$$\tau_{diff} = \frac{R^2}{D_{D,ave}} \tag{13}$$

where R is microparticle radius and $D_{D,ave}$ is a time and radius-averaged drug diffusion coefficient since this value varies both in time and space during degradation, as explained above. Simulations allowed obtaining τ_{sol} values of 0.205 and 0.247 days, and τ_{diff} values of 17.141 and 25.185 days for 7.2 and 53 μm microspheres, respectively, in good accordance with the experimental data reported in Figure 3. With the characteristic diffusion time much larger than the solubilization one, drug release is first of all determined by diffusion phenomena. Increasing solubilization constant $k_{C,D}^{int}$, implies a τ_{sol} decrease, but since diffusion still plays the rate-determining step in drug release, this dissolution enhancement has no effect on the final behavior.

As recently reviewed,[49] although drug solubilization actually occurs and constitutes a physical step in the involved phenomena, drug release can be described by means of the diffusion equation only. This implies that, in the resulting system, eqs 6.a and 6.b are substituted by the following expressions:

$$\frac{\partial C_D}{\partial t} = \frac{1}{r^2}\frac{\partial}{\partial r}\left(D_{D,eff} r^2 \frac{\partial C_D}{\partial r}\right) \tag{14}$$

$$D_{D,eff} = D_{D,eff}^0 \exp\left[2.5\left(1 - \frac{MW_n(t, r)}{MW_n(t = 0)}\right)^{0.5}\right] \tag{15}$$

where C_D is drug concentration and $D_{D,eff}$ is the effective drug diffusion coefficient, expressed with the same formalism represented by eq 9, and here reported for the sake of completeness (eq 15). Such approach provides a lumped description of drug solubilization and diffusion. In particular, the diffusion coefficient, which appears in eqs 14 and 15, is not strictly a diffusivity value because it implicitly accounts for the solubilization effects, but an overall effective value.

A quantitative evaluation can be seen in Figure 5, where the detailed and the simplified drug release predictions (accounting both solubilization and diffusion, and diffusion only, respectively) are compared along with experimental data.

It can be seen that both methods provide a good agreement with experimental data and are thus essentially equivalent; in particular, $D_{D,eff}^0$ values are equal to 9.146×10^{-15} and 3.107×10^{-13} cm^2 s^{-1} for 7.2 and 53 μm systems, respectively, against diffusivity values equal to 3.972×10^{-13} and 1.324×10^{-12} cm^2 s^{-1} referred to the detailed model. Effective diffusion coefficients values are lower since they also contain dissolution dynamics; such trend has been observed also by Siepmann et al.[49] Notably, the lumped diffusivity value becomes closer to the diffusion coefficient related to the dissolution−diffusion approach as size increases; for larger microspheres the role of diffusion is more important than the dissolution one since the diffusive paths are longer.

From a physical point of view, the agreement with experimental data means that, for the system under investigation, the rate-determining step in drug release is the active ingredient diffusion through the device (as shown by the characteristic times analysis), and the dissolution can thus be safely neglected. Although this approach offers a simplified view of the involved phenomena, it requires only one fitting parameter (the effective diffusion coefficient) and hence reduces model complexity. However, a detailed model is required in order to achieve an exhaustive understanding of the involved phenomena, their mutual synergy, and the role of each physical step.

Another meaningful analysis concerning transport phenomena mechanisms involves the influence of the mass transfer coefficient $k_{C,D}^{ext}$. Simulations showed that increasing or decreasing $k_{C,D}^{ext}$ up to 2 orders of magnitude has no influence on the drug release rate, as shown in Figure 6, where release rates computed changing $k_{C,D}^{ext}$ are superimposed. Such evidence has a physical meaning, that is, drug diffusion is confirmed to be the determining step for drug release. This assumption is consistent with the results obtained by Siepmann and co-workers.[44]

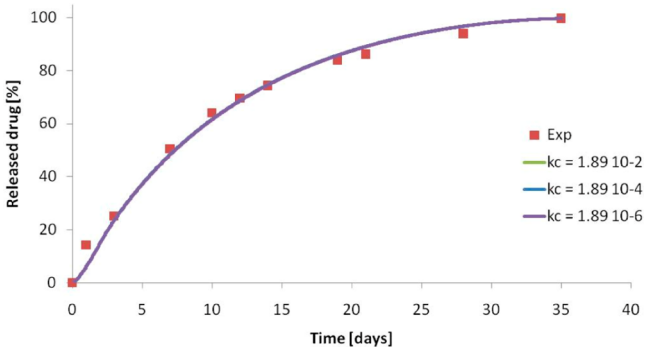

Figure 6. Experimental (squares) and computed (continuous lines) drug release from 53 μm lidocaine-loaded microparticles at different $k_{C,D}^{ext}$ values. Experimental data taken from Siepmann et al.[44]

Such evidence can be again explained in terms of characteristic times; the mass transfer characteristic time τ_{mt} can be defined as follows:

$$\tau_{mt} = \frac{1}{k_{C,D}^{ext} a} \tag{16}$$

where a is specific surface, that is, the ratio between microsphere surface and volume. Focusing on the example presented in Figure 5, τ_{mt} values range from 9.363×10^{-2} to 9.363×10^{2} s (less than 1 day, depending on $k_{C,D}^{ext}$ value), against a characteristic diffusion time equal to 25.162 days, much higher than the mass transfer one. This approach thus provides a quantitative proof of the dominant role of diffusion in drug release for the system under investigation. For the sake of completeness, the τ_{mt} value referred to 7.2 μm system is equal to 0.173 s, confirming the validity of the obtained results also for smaller particles.

Ibuprofen-Loaded Microparticles. Klose et al.[45] expanded the work of Siepmann and co-workers[44] by synthesizing ibuprofen-loaded PLGA microparticles having different radii, ranging from 13 to 57.5 μm; they described degradation through a pseudo first order kinetics, evidencing an autocatalytic effect since the fitted kinetic constants increase as particle size increases. The here proposed model can satisfactorily describe the microparticles' molecular weight loss, as shown in Figure 7.

The kinetic constant values range from 2.016×10^{-3} to 3.364×10^{-3} cm^6 mol^{-2} s^{-1}, similarly to lidocaine-loaded microparticles, still suggesting the attainment of a limited drug influence on device degradation and the importance of autocatalytic effect, which increases as size increases.

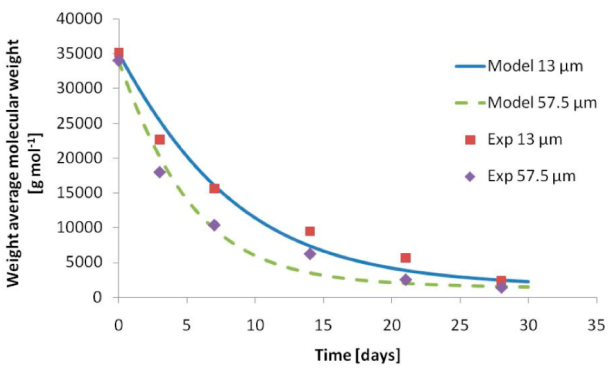

Figure 7. Experimental (squares) and predicted (continuous and dashed lines) molecular weight loss for ibuprofen-loaded microparticles. Size values refer to microsphere radii. Experimental data taken from Klose et al.[45]

Furthermore, for drug release, the model provides a good agreement with experimental data. Again, for the sake of clarity, only release profiles related to the smallest and the biggest sizes are here presented, while the remaining calculations (related to the remaining particle sizes) are reported in the Supporting Information.

Solubilization constant values equal to 4.635×10^{-2} and 2.896×10^{-2} s^{-1} and initial diffusion coefficients values equal to 3.424×10^{-10} and 3.926×10^{-9} cm^2 s^{-1} have been obtained for 13 and 57.5 μm microparticles, respectively, from experimental data fitting (Figure 8). As previously seen for lidocaine-loaded particles, solubilization constants result very close to each other for the differently sized particles, indicating a similar drug dispersion. Diffusion coefficients increase as size increases, again as seen for lidocaine-loaded microparticles.

A comparison with lidocaine-loaded microspheres leads to interesting results. Even though lidocaine and ibuprofen have comparable molecular weights and steric hindrance and the initial drug loading is the same for both devices, ibuprofen release occurs more rapidly than the lidocaine one. Solubilization constants for ibuprofen are about 3 orders of magnitude larger than the ones obtained for lidocaine, and this trend may be related to drug dispersion. In order to explain the observed trend, it may be assumed that in ibuprofen-loaded particles the drug is dispersed through a huge number of small crystallites, which possess a high specific surface promoting dissolution. Lidocaine instead leads to a reduced number of bigger crystallites, thus causing a slower drug solvation.

The diffusion coefficients trend can be explained considering the drug solubilization limit; such value is equal to 2.791×10^{-5} mol cm^{-3} for lidocaine[51] and 1.170×10^{-7} mol cm^{-3} for ibuprofen.[52] This means that, in water-filled pores, drug diffusion occurs in a more diluted solution and thus diffusion is faster. This also suggests that drug/polymer interactions, which may take place as drug diffuses, cannot entirely explain the different release dynamics. The obtained ibuprofen diffusion coefficients values are consistent since they are about 3 orders of magnitude lower than ibuprofen self-diffusion coefficient in water, equal to 5.47×10^{-6} cm^2 s^{-1}.[55]

The description of drug release by means of the diffusion equation only, and thus neglecting dissolution, provides a good agreement with experimental data (Figure 9).

It can be seen that both simplified and detailed models provide a good agreement with experimental data. In particular, $D_{D,eff}^{0}$ values equal to 3.043×10^{-13} and 2.185×10^{-12} cm^2 s^{-1} have been obtained for 13 and 57.5 μm microspheres, respectively. Characteristic time analysis showed that also for ibuprofen-loaded microparticles diffusion plays a key role during the release of drug.

Paclitaxel-Loaded Microparticles. Elkharratz et al.[43] synthesized and characterized paclitaxel-loaded microspheres. In particular, they evaluated the effect of *N*,*N*-diethylnicotinamide (DENA) in the surrounding medium on both polymer degradation and drug release. This ingredient enhances drug solubility up to 2000 times,[43] allowing to overcome the problem of low paclitaxel solubility in water environment (about 0.6×10^{-6} mol cm^{-3}[53]). Experimental data showed that the presence of DENA in the surrounding medium accelerates not only paclitaxel release but also molecular weight decrease. This is due to the DENA catalytic effect[43] since hydrolysis is also catalyzed by bases.[10] The model does not take explicitly into account the

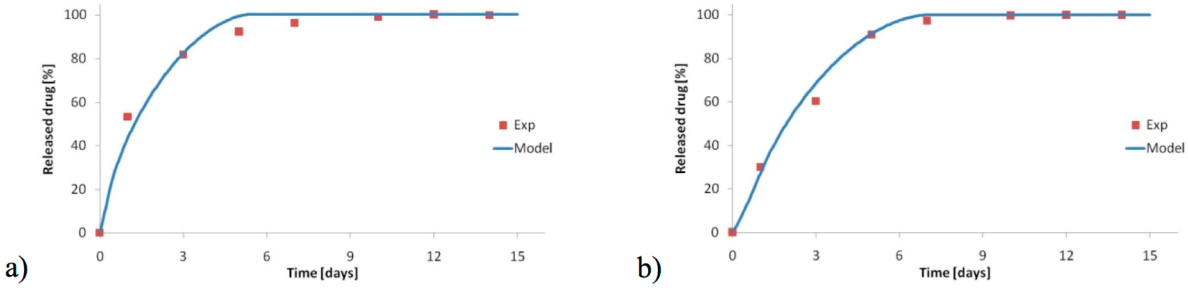

Figure 8. Experimental (squares) and predicted (continuous lines) release profiles for 13 μm microparticles (a) and 57.5 μm microparticles (b). Experimental data taken from Klose et al.[45]

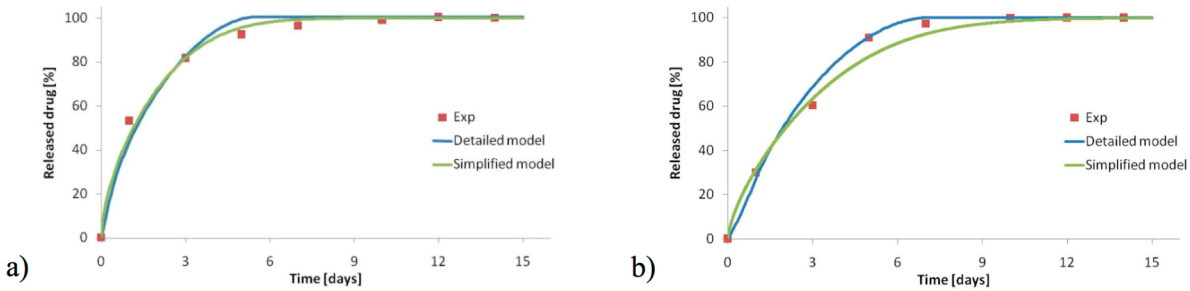

Figure 9. Comparison between detailed and simplified drug release description for 13 μm microparticles (a) and 57.5 μm microparticles (b). Experimental data (squares) taken from Klose et al.[45]

presence of DENA in the surrounding medium, but its effect is accounted for in the estimated kinetic constant, similarly to the drug effect on degradation, as discussed above. Simulations showed a good agreement with experimental data (Figure 10).

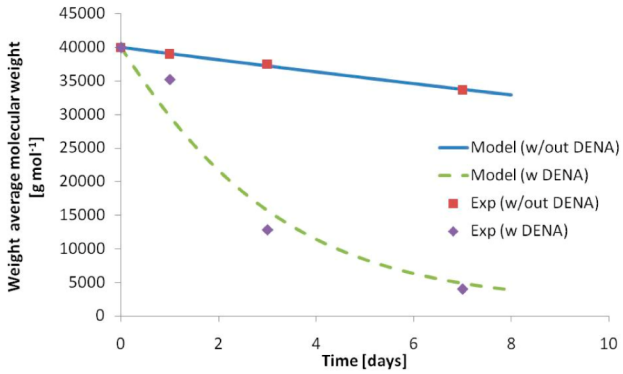

Figure 10. Experimental (squares) and predicted (continuous and dashed lines) molecular weight loss with and without *N,N*-diethylnicotinamide (DENA) in the surrounding medium. Experimental data taken from Elkharratz et al.[43]

The kinetic constant, when DENA is added to the surrounding medium, is equal to 5.571×10^{-3} cm^6 mol^{-2} s^{-1}, while a value equal to 4.062×10^{-4} cm^6 mol^{-2} s^{-1} is obtained for sole buffer saline solution medium. Such evaluation suggests that polymer degradation is about ten times faster when DENA is used to increase paclitaxel solubility.[53]

For drug release, the here proposed model provides only a reasonable agreement with experimental data, with both dissolution−diffusion and diffusion approaches. In order to overcome such limit, calculations have been performed assuming a nonuniform initial drug distribution; there is evidence that, in polymeric microparticles, highly hydrophobic drugs (such as paclitaxel) are not uniformly dispersed but are mainly located in the device core. Raman et al.,[56] e.g., studied piroxicam distribution in PLGA microparticles, highlighting a nonhomogeneous piroxicam distribution in 50 μm devices. The initial paclitaxel distribution has been described as follows:

$$C_D(r, t = 0) = C_{D,0}\left(\exp\left(-\alpha\frac{r}{R}\right) + \beta\right) \tag{17}$$

where α and β are dimensionless arbitrary parameters, R is the microparticle radius, and $C_{D,0}$ is a parameter computed by imposing that the integral of eq 17 over the microparticle volume is equal to the experimental drug loading:

$$M_D = 4\pi C_{D,0}\int_0^R \left(\exp\left(-\alpha\frac{r}{R}\right) + \beta\right) r^2 dr \tag{18}$$

where M_D is the initial drug amount, in molar terms, in the microsphere. A paclitaxel distribution mainly located in the particle center can be reasonably described with α and β values equal to 30 and 1.2×10^{-4}, respectively (Figure 11a). For the sake of simplicity, calculations made adopting such initial drug distribution have been carried out using the diffusion approach, thus assuming that drug dissolution is not the determining step in drug release. Since the active ingredient dispersion is not uniform, it is reasonable to assume that crystallite number and dimension (and thus, specific surface) strongly vary with drug concentration. Thus, dissolution cannot be described adopting a constant value of $k_{C,D}^{int}$, but a functional dependence of this parameter with respect to drug concentration or crystallite characteristic dimension should be given.

As shown in Figure 11b, a nonuniform drug distribution allowed reproducing the experimental release rate; the good agreement with experimental data confirms that diffusion is still the determining step in drug release, and it underlines that the initial drug distribution plays also an important role in the overall device behavior.

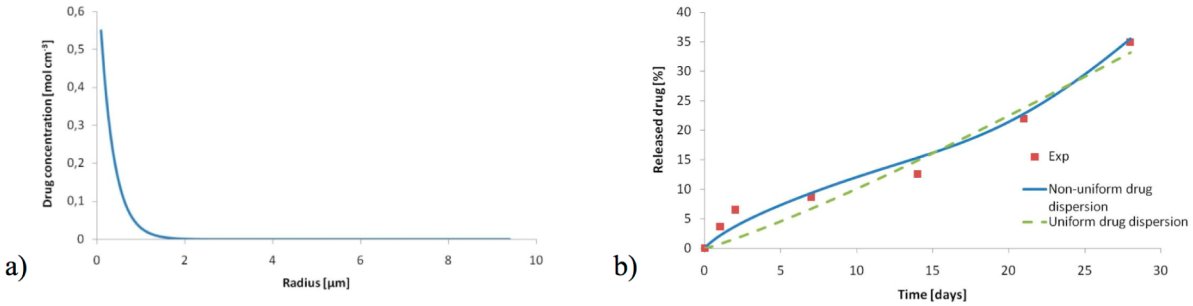

Figure 11. Nonuniform drug distribution with respect to particle radius (a) and comparison between predicted (continuous and dashed lines) and experimental paclitaxel release (squares) from 18.8 μm microparticles (b). Experimental data taken from Elkharratz et al.[43]

Simulations have been performed using a paclitaxel effective diffusion coefficient equal to 7.04×10^{-15} cm^2 s^{-1}. It should be highlighted that α and β values are arbitrarily chosen since the effective drug distribution in the microspheres was not investigated by Elkharratz and co-workers. However, this does not affect the main result of this analysis, that is, the influence of drug distribution on release profile. As shown in Figure 11b, the predicted release rate trend is in good agreement with the experimental one when an initial nonuniform drug distribution is adopted, while a uniform distribution is not able to reproduce the experimental evidence.

In order to investigate the effect of a nonuniform drug distribution on release rate, additional simulations have been carried out varying α and β (compare to Table 3); for the sake of simplicity, $D_{D,eff}^0$ has been kept constant and equal to 7.04×10^{-15} cm^2 s^{-1}, as previously found.

Table 3. Values of α and β Used in Simulations

simulation	α	β
1	15	1.2×10^{-3}
2	7	1.2×10^{-2}
3	40	1.2×10^{-5}

Notably, calculations show that the initial drug distribution (Figure 12a) has a significant effect on drug release (Figure 12b); the model thus suggests that an experimental control of drug dispersion could be used as a device design parameter in order to properly tune the release of active ingredients.

Theoretical Predictions. In this framework, the model has been validated only by means of fitting from each set of experimental data, and thus could be considered empirical or semiempirical although it derives from a first-principles approach.

For the sake of completeness, it should be pointed out that fitted parameters are hydrolysis kinetic constant k_d, drug diffusion coefficient before degradation onset D_D^0, and solubilization constant $k_{C,D}^{int}$. When dissolution dynamics are neglected, the model requires only two fitted parameters, i.e., k_d and the effective drug diffusion coefficient before degradation onset $D_{D,eff}^0$. The remaining parameters represent physical properties (such as polymer density) or reasonable estimations (such as water diffusion coefficient within the polymeric matrix).

First of all, it can be seen that hydrolysis kinetic constants values for drug-free microparticles vary in a limited range; using a unique average k_d value (1.53×10^{-3} mol^{-2} cm^6 s^{-1}) leads to good agreement with experimental data for all considered sizes, which means that autocatalysis behavior is reproduced at least from a qualitative point of view, as shown in Figure 13.

This is no longer true when dealing with drug-loaded microparticles since hydrolysis kinetic constants have a non-negligible variation as radius increases, suggesting that the loaded drug can influence degradation behavior. The effect of the active principle on the overall hydrolysis process is not explicitly taken into account in population balances, and the observed differences within k_d values could be expected. In this situation, the model validity can lie in the prediction of variable trends, which can be used in order to make theoretical predictions, as demonstrated, e.g., by Faisant et al.[57]

Kinetic constants for drug-loaded particles have been fitted from three different experimental data sets among the four ones available from the manuscript of Siepmann et al.,[44] in order to determine a quantitative relationship between k_d and particle size (Figure 14a). A kinetic constant value equal to 2.74×10^{-3} mol^{-2} cm^6 s^{-1} is obtained for the fourth data set related to 37 μm particles and used for theoretical prediction concerning polymer degradation, which is in good agreement with experimental data (Figure 14b).

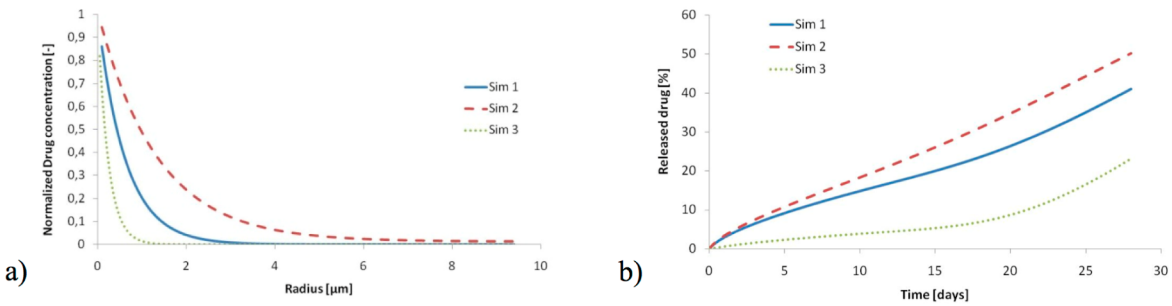

Figure 12. Nonuniform normalized drug distributions with respect to particle radius (a) and predicted paclitaxel release from 9.4 μm microparticles (b).

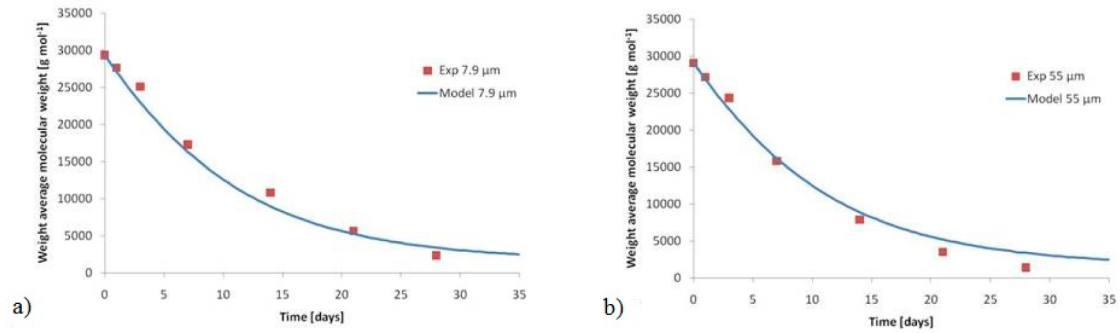

Figure 13. Experimental (squares) and predicted (continuous lines) time evolution of weight-average molecular weight for 7.9 μm (a) and 55 μm (b) microparticles using a unique average k_d value equal to 1.53×10^{-3} mol^{-2} cm^6 s^{-1}. Size values refer to microsphere radii. Experimental data taken from Siepmann et al.[44]

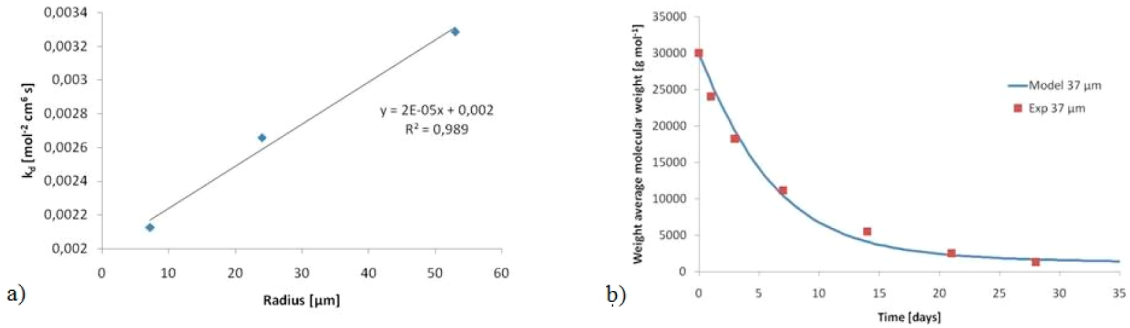

Figure 14. Size dependence of hydrolysis constant for drug-loaded devices (a) and comparison between experimental (squares) and predicted (continuous line) time evolution of weight-average molecular weight for 37 μm particles. Experimental data taken from Siepmann et al.[44]

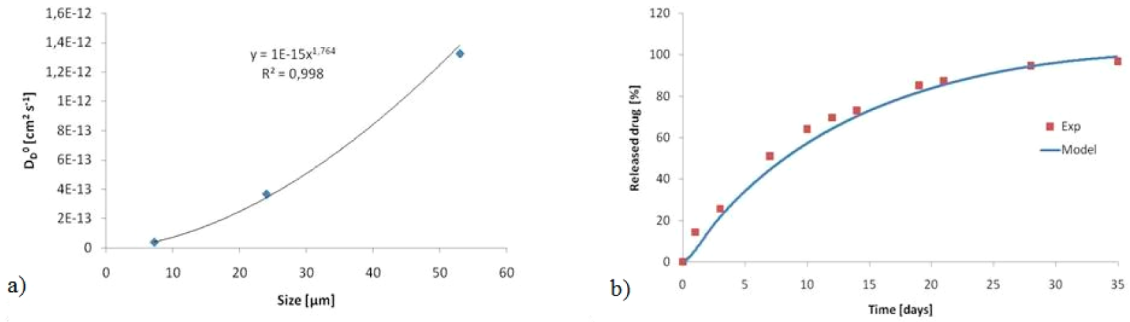

Figure 15. Size dependence of drug diffusion coefficient before degradation onset (a) and comparison between experimental (squares) and predicted (continuous line) time evolution of drug release profile for 37 μm particles. Experimental data taken from Siepmann et al.[44]

The same procedure can be applied for drug release predictions: three experimental data sets are used in order to establish a quantitative relationship between the drug diffusion coefficient before degradation onset D_D^0 and predict the value for the fourth set (Figure 15a). Dissolution constant has been estimated as an average value since it varies in a limited range and does not show a strong size dependence. Thus, 37 μm microparticle simulation has been performed using D_D^0 and $k_{C,D}^{int}$ values equal to 5.839×10^{-13} cm^2 s^{-1} and 5.047×10^{-5} s^{-1}, respectively.

As shown in Figure 15b, although the predicted release profile exhibits a slight underestimation of experimental data (data fitting for 37 μm microspheres would lead to a D_D^0 value equal to 8.048×10^{-13} cm^2 s^{-1}), the agreement can be considered satisfactory.

This confirms that the model is able to predict variable trend, allowing to make theoretical predictions for arbitrarily particle size values.

■ CONCLUSIONS

The present work has been devoted to the development and the validation of a mathematical model able to describe the behavior of drug-loaded polymeric microparticles, in terms of degradation and drug release. Polymer degradation has been characterized taking into account the autocatalytic effect due to the acidic environment within the device, while drug release has been described considering also the solubilization dynamics of drug crystallites.

The model derives from a first-principles approach: this means that every involved parameter has a physical meaning and can be robustly estimated from experimental data. Because of this, and thanks to a satisfactory validation, the here proposed model can

be employed to perform an *in silico* evaluation of the influence of the most relevant device design variables, becoming a valuable tool to optimize experimental activity. Moreover, the estimated parameters reflect the peculiarities of each system: a higher hydrolysis kinetic constant for drug-loaded devices, e.g., may suggest the presence of drug influence on polymer degradation, while different values of drug dissolution constant may indicate a different distribution of active pharmaceutical ingredient within the matrix, in terms of numbers and dimensions of crystallites.

The influence of estimated parameters has been properly discussed through a simple but effective analysis, carried out by means of characteristic times, highlighting the main role possessed by diffusion in the drug release process. The effect of a nonuniform initial drug distribution into the device has been proposed, in order to reproduce an experimental trend, which could not be satisfactorily predicted assuming a homogeneous active ingredient dispersion. From the authors' best knowledge, it is the first time that, in a mathematical modeling framework, the influence of initial drug dispersion on the release profile has been underlined.

Quantitative relationships between particles size and both hydrolysis kinetic constant and drug diffusion coefficient before degradation onset could be obtained for drug-loaded devices. Such relationships were used to make theoretical predictions of both device degradation and drug release kinetics, whose validity has been confirmed through a good agreement with experimental data.

■ ASSOCIATED CONTENT

Ⓢ Supporting Information

Model development, detailed boundary and initial conditions, error estimations, and plots and fitting parameters concerning all experimental data. This material is available free of charge via the Internet at http://pubs.acs.org.

■ AUTHOR INFORMATION

Corresponding Author

*Tel: +39 02 2399 3107. Fax: +39 02 2399 3180. E-mail: tommaso.casalini@mail.polimi.it.

Notes

The authors declare no competing financial interest.

■ REFERENCES

(1) Seyednejad, H.; Ghassemi, A. H.; van Nostrum, C. F.; Vermonden, T.; Hennink, W. E. Functional Aliphatic Polyesters for Biomedical and Pharmaceutical Applications. *J. Controlled Release* **2011**, *152* (1), 168−176.

(2) Ikada, Y.; Tsuji, H. Biodegradable Polyesters for Medical and Ecological Applications. *Macromol. Rapid Commun.* **2000**, *21* (3), 117−132.

(3) Nair, L. S.; Laurencin, C. T. Biodegradable Polymers as Biomaterials. *Prog. Polym. Sci.* **2007**, *32* (8−9), 762−798.

(4) Mohtaram, N. K.; Montgomery, A.; Willerth, S. M. Biomaterial-based Drug Delivery Systems for the Controlled Release of Neurotrophic Factors. *Biomed. Mater.* **2013**, *8* (2), 022001.

(5) Freiberg, S.; Zhu, X. Polymer Microspheres for Controlled Drug Release. *Int. J. Pharm.* **2004**, *282* (1−2), 1−18.

(6) Rui, J.; Dadsetan, M.; Runge, M. B.; Spinner, R. J.; Yaszemski, M. J.; Windebank, A. J.; Wang, H. Controlled Release of Vascular Endothelial Growth Factor Using Poly-lactic-co-glycolic Acid Microspheres: In Vitro Characterization and Application in Polycaprolactone Fumarate Nerve Conduits. *Acta Biomater.* **2012**, *8* (2), 511−518.

(7) de Boer, R.; Knight, A. M.; Spinner, R. J.; Malessy, M. J. A.; Yaszemski, M. J.; Windebank, A. J. In Vitro and in Vivo Release of Nerve Growth Factor from Biodegradable Poly-lactic-co-glycolic-acid Microspheres. *J. Biomed. Mater. Res., Part A* **2010**, *95A* (4), 1067−1073.

(8) Stevanovic, M.; Uskokovic, D. Poly(lactide-co-glycolide)-based Micro and Nanoparticles for the Controlled Drug Delivery of Vitamins. *Curr. Nanosci.* **2009**, *5* (1), 1−14.

(9) Patel, M. M.; Zeles, M. G.; Manning, M. C.; Randolph, T. W.; Anchordoquy, T. J. Degradation Kinetics of High Molecular Weight Poly (L-lactide) Microspheres and Release Mechanism of Lipid: DNA Complexes. *J. Pharm. Sci.* **2004**, *93* (10), 2573−2584.

(10) Alexis, F. Factors Affecting the Degradation and Drug-release Mechanism of Poly(lactic acid) and Poly[(lactic acid)-co-(glycolic acid)]. *Polym. Int.* **2005**, *54* (1), 36−46.

(11) Fredenberg, S.; Wahlgren, M.; Reslow, M.; Axelsson, A. The Mechanisms of Drug Release in Poly(lactic-co-glycolic acid)-based Drug Delivery Systems: A Review. *Int. J. Pharm.* **2011**, *415* (1−2), 34−52.

(12) Grassi, M.; Grassi, R.; Lapasin, R.; Colombo, I. *Understanding Drug Release and Absorption Mechanisms*; CRC Press: Boca Raton, FL, 2008.

(13) Li, S. M. Hydrolytic Degradation Characteristics of Aliphatic Polyesters Derived from Lactic and Glycolic Acids. *J. Biomed. Mater. Res.* **1999**, *48* (3), 342−353.

(14) Alexis, F.; Kumar Rath, S.; Venkatraman, S. Controlled Release from Bioerodible Polymers: Effect of Drug Type and Polymer Composition. *J. Controlled Release* **2005**, *102*, 333−344.

(15) Siegel, S. J.; Kahn, J. B.; Metzger, K.; Winey, K. I.; Werner, K.; Dan, N. Effect of Drug Type on the Degradation Rate of PLGA Matrices. *Eur. J. Pharm. Biopharm.* **2006**, *64* (3), 287−293.

(16) von Burkersroda, F.; Schedl, L.; Gopferich, A. Why Degradable Polymers Undergo Surface Erosion or Bulk Erosion. *Biomaterials* **2002**, *23* (21), 4221−4231.

(17) Grizzi, I.; Garreau, H.; Li, S.; Vert, M. Hydrolytic Degradation of Devices Based on Poly(DL-Lactic Acid) Size-Dependence. *Biomaterials* **1995**, *16* (4), 305−311.

(18) Versypt, A. N. F.; Pack, D. W.; Braatz, R. D. Mathematical Modeling of Drug Delivery from Autocatalytically Degradable PLGA Microspheres: A Review. *J. Controlled Release* **2013**, *165* (1), 29−37.

(19) Lauzon, M. A.; Bergeron, E.; Marcos, B.; Faucheux, N. Bone Repair: New Developments in Growth Factor Delivery Systems and Their Mathematical Modeling. *J. Controlled Release* **2012**, *162* (3), 502−520.

(20) Lao, L. L.; Peppas, N. A.; Boey, F. Y. C.; Venkatraman, S. S. Modeling of Drug Release from Bulk-degrading Polymers. *Int. J. Pharm.* **2011**, *418* (1), 28−41.

(21) Sackett, C. K.; Narasimhan, B. Mathematical Modeling of Polymer Erosion: Consequences for Drug Delivery. *Int. J. Pharm.* **2011**, *418* (1), 104−114.

(22) Zhang, M. P.; Yang, Z. C.; Chow, L. L.; Wang, C. H. Simulation of Drug Release from Biodegradable Polymeric Microspheres with Bulk and Surface Erosions. *J. Pharm. Sci.* **2003**, *92* (10), 2040−2056.

(23) Wang, Y.; Pan, J. Z.; Han, X. X.; Sinka, C.; Ding, L. F. A Phenomenological Model for the Degradation of Biodegradable Polymers. *Biomaterials* **2008**, *29* (23), 3393−3401.

(24) Antheunis, H.; van der Meer, J. C.; de Geus, M.; Heise, A.; Koning, C. E. Autocatalytic Equation Describing the Change in Molecular Weight during Hydrolytic Degradation of Aliphatic Polyesters. *Biomacromolecules* **2010**, *11* (4), 1118−1124.

(25) Antheunis, H.; van der Meer, J. C.; de Geus, M.; Kingma, W.; Koning, C. E. Improved Mathematical Model for the Hydrolytic Degradation of Aliphatic Polyesters. *Macromolecules* **2009**, *42* (7), 2462−2471.

(26) Rothstein, S. N.; Federspiel, W. J.; Little, S. R. A Unified Mathematical Model for the Prediction of Controlled Release from Surface and Bulk Eroding Polymer Matrices. *Biomaterials* **2009**, *30* (8), 1657−1664.

(27) Chen, Y. H.; Zhou, S. W.; Li, Q. Mathematical Modeling of Degradation for Bulk-Erosive Polymers: Applications in Tissue Engineering Scaffolds and Drug Delivery Systems. *Acta Biomater.* **2011**, *7* (3), 1140−1149.

(28) Siepmann, J.; Faisant, N.; Benoit, J. P. A New Mathematical Model Quantifying Drug Release from Bioerodible Microparticles Using Monte Carlo Simulations. *Pharm. Res.* **2002**, *19* (12), 1885−1893.
(29) Barat, A.; Crane, M.; Ruskin, H. J. Quantitative Multi-agent Models for Simulating Protein Release From PLGA Bioerodible Nano- and Microspheres. *J. Pharm. Biomed.* **2008**, *48* (2), 361−368.
(30) Arosio, P.; Busini, V.; Perale, G.; Moscatelli, D.; Masi, M. A New Model of Resorbable Device Degradation and Drug Release. Part I: Zero Order Model. *Polym. Int.* **2008**, *57* (7), 912−920.
(31) Perale, G.; Arosio, P.; Moscatelli, D.; Barri, V.; Muller, M.; Maccagnan, S.; Masi, M. A New Model of Resorbable Device Degradation and Drug Release: Transient 1-dimension Diffusional Model. *J. Controlled Release* **2009**, *136* (3), 196−205.
(32) Batycky, R. P.; Hanes, J.; Langer, R.; Edwards, D. A. A Theoretical Model of Erosion and Macromolecular Drug Release from Biodegrading Microspheres. *J. Pharm. Sci.* **1997**, *86* (12), 1464−1477.
(33) Perale, G.; Casalini, T.; Barri, V.; Muller, M.; Maccagnan, S.; Masi, M. Lidocaine Release From Polycaprolactone Threads. *J. Appl. Polym. Sci.* **2010**, *117* (6), 3610−3614.
(34) Casalini, T.; Masi, M.; Perale, G. Drug Eluting Sutures: A Model For In Vivo Estimations. *Int. J. Pharm.* **2012**, *429* (1−2), 148−157.
(35) Nishida, H.; Yamashita, M.; Nagashima, M.; Hattori, N.; Endo, T.; Tokiwa, Y. Theoretical Prediction of Molecular Weight on Autocatalytic Random Hydrolysis of Aliphatic polyesters. *Macromolecules* **2000**, *33* (17), 6595−6601.
(36) van Nostrum, C. F.; Veldhuis, T. F. J.; Bos, G. W.; Hennink, W. E. Hydrolytic Degradation of Oligo(lactic acid): a Kinetic and Mechanistic Study. *Polymer* **2004**, *45* (20), 6779−6787.
(37) Arifin, D. Y.; Lee, L. Y.; Wang, C. H. Mathematical Modeling and Simulation of Drug Release From Microspheres: Implications to Drug Delivery Systems. *Adv. Drug Delivery Rev.* **2006**, *58* (12−13), 1274−1325.
(38) Siepmann, J.; Siepmann, F. Modeling of Diffusion Controlled Drug Delivery. *J. Controlled Release* **2012**, *161* (2), 351−362.
(39) Faisant, N.; Siepmann, J.; Benoit, J. P. PLGA-based Microparticles: Elucidation of Mechanisms and a New, Simple Mathematical Model Quantifying Drug Release. *Eur. J. Pharm. Sci.* **2002**, *15* (4), 355−366.
(40) Saralidze, K.; Koole, L. H.; Knetsch, M. L. W. Polymeric Microspheres for Medical Applications. *Materials* **2010**, *3* (6), 3537−3564.
(41) Wischke, C.; Schwendeman, S. P. Principles of Encapsulating Hydrophobic Drugs in PLA/PLGA Microparticles. *Int. J. Pharm.* **2008**, *364* (2), 298−327.
(42) Soares, J. S.; Zunino, P. A Mixture Model for Water Uptake, Degradation, Erosion and Drug Release from Polydisperse Polymeric Networks. *Biomaterials* **2010**, *31* (11), 3032−3042.
(43) Elkharraz, K.; Faisant, N.; Guse, C.; Siepmann, F.; Arica-Yegin, B.; Oger, J. M.; Gust, R.; Goepferich, A.; Benoit, J. P.; Siepmann, J. Paclitaxel-loaded Microparticles and Implants for the Treatment of Brain Cancer: Preparation and Physicochemical Characterization. *Int. J. Pharm.* **2006**, *314* (2), 127−136.
(44) Siepmann, J.; Elkharraz, K.; Siepmann, F.; Klose, D. How Autocatalysis Accelerates Drug Release from PLGA-based Microparticles: A Quantitative Treatment. *Biomacromolecules* **2005**, *6* (4), 2312−2319.
(45) Klose, D.; Siepmann, F.; Elkhamz, K.; Siepmann, J. PLGA-based Drug Delivery Systems: Importance of the Type of Drug and Device Geometry. *Int. J. Pharm.* **2008**, *354* (1−2), 95−103.
(46) Ford, A. N.; Pack, D. W.; Braatz, R. D. Multi-Scale Modeling of PLGA Microparticle Drug Delivery Systems. *Comput-Aided Chem. Eng.* **2011**, *29*, 1475−1479.
(47) Ramkrishna, D. *Population Balances*; Academic Press: San Diego, CA, 2000.
(48) Rossi, F.; Casalini, T.; Raffa, E.; Masi, M.; Perale, G. Bioresorbable Polymer Coated Drug Eluting Stent: A Model Study. *Mol. Pharmaceutics* **2012**, *9* (7), 1898−1910.
(49) Siepmann, J.; Siepmann, F. Mathematical Modeling of Drug Dissolution. *Int. J. Pharm.* **2013**, *453* (1), 12−24.
(50) Bird, R. B.; Stewart, W. E.; Lightfoot, E. N. *Transport Phenomena*, 2nd; J. Wiley: New York, 2002; p xii.
(51) Loftsson, T.; Hreinsdottir, D. Determination of Aqueous Solubility by Heating and Equilibration: A Technical Note. *AAPS PharmSciTech* **2006**, *7* (1), E29−E32.
(52) Garzon, L. C.; Martinez, F. Temperature Dependence of Solubility for Ibuprofen in Some Organic and Aqueous Solvents. *J. Solution Chem.* **2004**, *33* (11), 1379−1395.
(53) Singla, A. K.; Garg, A.; Aggarwal, D. Paclitaxel and Its Formulations. *Int. J. Pharm.* **2002**, *235* (1−2), 179−192.
(54) LeVeque, R. J. *Finite Difference Methods for Ordinary and Partial Differential Equations*; Society for Industrial and Applied Mathematics: Philadelphia, PA, 2007.
(55) Derrick, T. S.; McCord, E. F.; Larive, C. K. Analysis of Protein/Ligand Interactions with NMR Diffusion Measurements: The Importance of Eliminating the Protein Background. *J. Magn. Reson.* **2002**, *155* (2), 217−225.
(56) Raman, C.; Berkland, C.; Kim, K.; Pack, D. W. Modeling Small-molecule Release from PLG Microspheres: Effects of Polymer Degradation and Nonuniform Drug Distribution. *J. Controlled Release* **2005**, *103* (1), 149−158.
(57) Faisant, N.; Siepmann, J.; Richard, J.; Benoit, J. P. Mathematical Modeling of Drug Release from Bioerodible Microparticles: Effect of Gamma-irradiation. *Eur. J. Pharm. Biopharm.* **2003**, *56* (2), 271−279.